

CrystEngComm

Accepted Manuscript



This is an *Accepted Manuscript*, which has been through the Royal Society of Chemistry peer review process and has been accepted for publication.

Accepted Manuscripts are published online shortly after acceptance, before technical editing, formatting and proof reading. Using this free service, authors can make their results available to the community, in citable form, before we publish the edited article. We will replace this *Accepted Manuscript* with the edited and formatted *Advance Article* as soon as it is available.

You can find more information about *Accepted Manuscripts* in the [Information for Authors](#).

Please note that technical editing may introduce minor changes to the text and/or graphics, which may alter content. The journal's standard [Terms & Conditions](#) and the [Ethical guidelines](#) still apply. In no event shall the Royal Society of Chemistry be held responsible for any errors or omissions in this *Accepted Manuscript* or any consequences arising from the use of any information it contains.

Two Manganese-amine Complexes Incorporated Thioantimonate Exhibiting Diversiform Roles of Amine-Ligands

Cheng-Yang Yue,^a Xiao-Wu Lei,^{a,b*} Hui-Ping Zang,^a Xiu-Rong Zhai,^a

Li-Juan Feng^a, Zhi-Fei Zhao,^a Jian-Qiang Zhao,^a Xin-Yue Liu^a

^a*Key Laboratory of Inorganic Chemistry in Universities of Shandong, Department of Chemistry and Chemical Engineering, Jining University, Qufu, Shandong, 273155, China*

^b*State Key Laboratory of Crystal Materials, Institute of Crystal Materials, Shandong University, Jinan, Shandong, 250100, China*

**Corresponding author: Xiao-Wu Lei*

E-mail address: xwlei_jnu@163.com

Abstract Two manganese-amine complexes incorporated thioantimonate, namely, $(\text{dienH}_3)[(\text{dienH})\text{MnSb}_8\text{S}_{15}]\cdot\text{H}_2\text{O}$ (dien = diethylenetriamine) (**1**) and $[\text{Mn}(\text{teta})(\text{H}_2\text{O})_2]_2[\text{Mn}(\text{tren})]_2\text{Sb}_3\text{S}_{12}\cdot\text{H}_3\text{O}$ (**2**, tetra = triethylenetetramine, tren = tris(2-aminoethyl)amine), have been solvothermally synthesized and structurally characterized. Interestingly, organic amines show diversiform structure-directing actions in the title compounds. In compound **1**, two dien molecules feature partial coordination mode to Mn^{2+} ion and protonated cations, respectively, and compound **2** contain mixed tetradentate tren and tetra chelating amines. The optical properties, thermal stabilities and magnetic properties have also been studied.

Introduction

In the past several decades, thioantimonates have drawn enormous interest because of their fascinating structural diversity and topologies, and potential applications in many areas such as optical, electronic and catalytic materials.¹⁻⁶ On the one hand, the antimony atom is favor to feature wide range of coordination numbers from 3 to 6, which would self-condense to lead to the formation of new secondary building units (SBUs) giving rise to novel thioantimonates with remarkable structures. On the other hand, the stereochemically active lone pair of antimony(III) is likely to induce structures with noncentrosymmetric or even chiral structures resulting in interesting physical properties, such as second-harmonic generation, enantioselective separation and catalysis.

Since the cobalt thioantimonate complex of $[\text{Co}(\text{en})_3]\text{CoSb}_4\text{S}_8$ was prepared in ethylenediamine (en) under mild solvothermal condition in 1996, solvothermal reaction in polyamine solution has become a versatile route for synthesizing main group thioantimonate.⁷ The chelating amine is not only an excellent solvent for solvothermal synthesis and reducing agent reacting with chalcogen elements, but also perform as protonated cations or *in situ* chelate transitional (or lanthanide) metal ions forming large $[\text{M}(\text{amine})_x]^{n+}$ complex counterions to stabilize chalcogenide anionic frameworks.⁸⁻¹¹ Now, the

protonated amine cations and transitional metal (TM) complexes have been widely used as structure-directing reagents, templates or counterions in the syntheses of thioantimonate.¹²⁻¹⁸ Generally speaking, the bi- and tridentate chelate amine, such as en and dien, usually preferably coordinate to the TM ions to form saturated hexa-coordinated complex as counter cations, which prevent the TM amine complexes form bonding with S atoms of thioantimonate anions, such as $[\text{Mn}(\text{en})_3]\text{Sb}_2\text{S}_5$, $[\text{Co}(\text{en})_3]\text{Sb}_{12}\text{S}_{19}$, $[\text{Ni}(\text{dien})_2]_3[\text{Sb}_3\text{S}_6]_2$, $[\text{Ni}(\text{dien})_2]_2\text{Sb}_4\text{S}_9$ and so on.¹⁹⁻²⁷ Contrarily, tetra- or pentadentate chelating amines, such as teta, tren or tepa (tepa = tetraethylenepentamine), usually coordinate to TM ions to form unsaturated complexes acting as structure direct agents, which can effectively incorporate anionic frameworks to form inorganic–organic hybrid thioantimonate.²⁸⁻³⁰ At the same time, the TM complexes may transfer the electronic, optical, and magnetic properties into the host inorganic framework, which also provide complementary properties and synergistic effects.

It is reported that in the chalcogenidometalates synthesized containing bi- or tridentate chelate amine solvent (en and dien, etc), the transitional metals trend to form saturated $[\text{TM}(\text{en})_3]$ or $[\text{TM}(\text{dien})_2]$ complexes due to their strong stabilities, and there are only a few reports on unsaturated $[\text{TM}(\text{en})_2]^{2+}$ or $[\text{TM}(\text{dien})]^{2+}$ units linking the chalcogen atoms to form hydrid chalcogenides.³¹ Furthermore, most of the chalcogenides are oriented by only one type of balanced cations, and examples simultaneously containing mixed TM complexes or protonated amines as multi-counterions are still scarce. Here, we present the solvothermal syntheses and characterizations of two organic–inorganic hybrid thioantimonates, $(\text{dienH}_3)[(\text{dienH})\text{MnSb}_8\text{S}_{15}] \cdot \text{H}_2\text{O}$ (**1**) and $[\text{Mn}(\text{teta})(\text{H}_2\text{O})_2]_2[\text{Mn}(\text{tren})]_2\text{Sb}_3\text{S}_{12} \cdot \text{H}_3\text{O}$ (**2**), in which the chelating amine feature diversiform structure-directing actions. The structure of compound **1** simultaneity contains protonated amine of $[\text{dienH}_3]^{3+}$ and unsaturated $[\text{Mn}(\text{dienH})]^{3+}$ complex, and compound **2** includes $[\text{Mn}(\text{teta})(\text{H}_2\text{O})_2]^{2+}$ complex and 1D $[\text{Mn}(\text{tren})]^{2+}$ chain.

Experimental

Materials and Instruments. All analytical grade chemicals were obtained commercially and used without further purification. C, H and N analyses were obtained on using a PE2400 II elemental

analyzer. Semi-quantitative energy dispersive X-ray analyses for Mn, Sb and S were performed on a JSM-6700F scanning electron microscope (SEM) equipped with an energy dispersive spectroscope (EDS) detector. Optical diffuse reflectance spectra were recorded using a computer-controlled PE Lambda 900 UV/vis spectrometer equipped with an integrating sphere in the wavelength range of 200–800 nm. FT-IR spectra were measured by Nicolet Magna-IR 550 spectrometer using KBr disks in the 4000–400 cm^{-1} range. Thermogravimetric analyses (TGA) were performed using a Mettler TGA/SDTA 851 thermal analyzer under N_2 atmosphere with heating rate of 10 $^\circ\text{C}\cdot\text{min}^{-1}$ in the temperature region of 30–800 $^\circ\text{C}$. X-ray diffraction (XRD) powder patterns were collected at room temperature on a X'Pert-Pro diffractometer using $\text{Cu K}\alpha$ radiation ($\lambda = 1.5406 \text{ \AA}$) in the 2θ range of 5–80 $^\circ$ with a step size of 0.04 $^\circ$ and 10 s/step counting time. Magnetic susceptibility measurements were performed on a Quantum Design PPMS-9T magnetometer at a field of 1000 Oe in the temperature range of 5–300 K.

Synthesis of compound 1. The reagents of $\text{Mn}(\text{CH}_3\text{COO})_2\cdot 4\text{H}_2\text{O}$ (0.0245 g, 0.1 mmol), Sb (0.0974 g, 0.8 mmol), S (0.0577 g, 1.8 mmol), diethylenetriamine (4 mL) and H_2O (1 mL) were sealed in a stainless steel reactor with a 15-mL Teflon liner, and then heated at 140 $^\circ\text{C}$ for 5 days and slowly cooled to room temperature at a rate of a controlled rate of 0.1 $^\circ\text{C}/\text{min}$. The product consisted of wine-colored plate-shaped crystals of **1** and small amount of an unknown black powder. The crystals of **1** were collected by hand under microscope, and washed with ethanol, dried, and then stored under vacuum (Yield: 0.104 g, 60% based on Sb). The compounds are stable under ambient conditions and insoluble in common solvents. Microprobe elemental analyses on clean surfaces of several single crystals of **1** gave Mn/Sb/S molar ratios of 0.91(8) : 8.21(2) : 15.18(5), which was in good agreement with the result determined by single crystal X-ray diffraction study. Elemental analysis for $\text{C}_8\text{H}_{32}\text{MnN}_6\text{OS}_{15}\text{Sb}_8$, Calcd: C 5.53%, H 1.85%, N 4.83%; Found: C 5.47%, H 1.79%, N 4.96%. IR (cm^{-1}): 3400 (s), 2920 (w), 2360 (w), 1640 (w), 1110 (w), 592 (w).

Synthesis of compound 2. A mixture of $\text{Mn}(\text{CH}_3\text{COO})_2\cdot 4\text{H}_2\text{O}$ (0.0490 g, 0.2 mmol), Sb (0.0244 g, 0.8 mmol), S (0.0256 g, 0.8 mmol) in 5 mL of triethylenetetramine (teta) aqueous solution (20% in

H₂O) was sealed in a stainless steel reactor with a 15-mL Teflon liner, and then heated at 140 °C for 5 days and slowly cooled to room temperature at a rate of a controlled rate of 0.1 °C/min. The product consisted of yellow block shaped crystals of **2** and small amount of an unknown black powder. The yellow crystals were selected by hand under microscope, washed with ethanol, dried, and then stored under vacuum (Yield: 0.0596 g, 13% based on Sb). The compounds are stable under ambient conditions and insoluble in common solvents. Microprobe elemental analyses on clean surfaces of several single crystals of **2** gave Mn/Sb/S molar ratios of 3.95(8) : 3.19(2) : 11.89(3), which was in good agreement with that determined by single crystal X-ray diffraction study. Anal. For C₂₄H₈₃Mn₄N₁₆O₅S₁₂Sb₃, Calcd: C 17.51 %, H 5.08 %, N 13.62%; Found: C 17.46 %, H 5.12 %, N 13.82%. IR (cm⁻¹): 3250 (s), 2870 (m), 1580 (w), 1420 (m), 995 (m), 627 (m).

Crystal Structure Determination. Single crystals of the title compounds were selected from the reaction products. Data collections for both compounds were performed with a Bruker SMART APEX-II CCD area detector on a D8 goniometer operated at room temperature. The structures were solved by using direct method (SHELXTL) and refined by full-matrix least-square technique.³² Non-hydrogen atoms were refined with anisotropic displacement parameters, and the hydrogen atoms bonded to C, N and O atoms were located at geometrically calculated positions and refined with fixed isotropic displacement parameters. Site occupancy refinements for both compounds indicated that all sites were fully occupied. Data collection and refinement parameters for the compounds are summarized in Table 1, and the important bond lengths are listed in Table 2, respectively. More details on the crystallographic studies are given in Supporting Information.

Results and Discussion

Protonated amines and transitional metal (TM) complexes have been widely used in the syntheses of inorganic–organic hybrid thioantimonates because of their excellent template or structure-directing effects. In this paper, we adopt tridentate chelating amine of dien and tetradentate chelating amine of tren and teta as ligands, which feature diversiform coordination models and structure-directing actions

in the title compounds. Interestingly, in the preparation of compound **2**, tetra serve as solvent but leading to mixed tetra and tren ligands in product, which maybe because commercial tetra contain a small amount of tren. Such phenomenon is also found in other resulting compounds.³³

Crystal Structure of 1. Single-crystal X-ray crystallography reveals that compound **1** crystallizes in the triclinic space group *P*-1 (No. 2) and features 1D [(dienH)MnSb₈S₁₅]³⁻ tubes built from 1D [Sb₆S₁₃] chains bridged by [Sb₂S₅] dimers and [(dienH)MnS₄] complexes via sharing corner S atoms, and (dienH)₃³⁺ act as counter cations to balance the negative charge of the anionic structure (Fig. 1). The asymmetric unit of **1** contains one crystallographically independent Mn²⁺, eight unique Sb³⁺, fifteen S²⁻, one H₂O and two dien molecules. The Sb(1), Sb(2), Sb(4) and Sb(5) atoms are surrounded by four S²⁻ ions with Ψ-[SbS₄] trigonal bipyramidal coordination geometries with two short (2.407(2)-2.525(2) Å) and two long (2.591(3)-2.872(2) Å) Sb-S distances, respectively, in which two long Sb-S bonds are nearly trans to each other; the fifth coordination site is occupied by the lone pair of the antimony(III). All the Sb(3), Sb(6), Sb(7) and Sb(8) atoms adopt SbS₃ trigonal-pyramidal coordination geometries with Sb-S bond lengths ranging from 2.359(3)-2.557(2) Å. The above Ψ-[SbS₄] trigonal bipyramids and [SbS₃] trigonal-pyramids have been reported in many thioantimonate, and these Sb-S bond lengths fall in the normal range values.¹⁹⁻²⁷ The Mn²⁺ ion is coordinated by two neighboring nitrogen donors from one dien ligand and four non-terminal S²⁻ ions (S(7), S(9), S(14) and S(15) atoms) from SbS₃ and SbS₄ units with distorted octahedral environment. Such partial coordination mode of dien ligand is similar to that of [Mn(dien)]MnSb₂S₅.³⁴ The Mn-S bond lengths fall in the range of 2.567(3)-2.726(3) Å, indicating strong covalent interactions. All the S²⁻ feature distinct metal linkers: S(4) link one Sb atom acting as terminal atoms, S(7), S(9) and S(15) ions connect with one Mn and two Sb atoms, respectively, and other S²⁻ ions bridge two Sb atoms.

Neighboring Ψ-Sb(1)S₄ and Ψ-Sb(2)S₄ trigonal bipyramids are condensed via edge-sharing to form a [Sb₂S₆] dimer, simultaneously, Ψ-Sb(4)S₄ and Ψ-Sb(5)S₄ constitute another type of [Sb₂S₆] dimer. These two types of [Sb₂S₆] dimers are alternately bridged by Sb(3)S₃ and Sb(6)S₃ trigonal-pyramids in turn via corner- and edge-sharing to form a 1D [Sb₆S₁₃] chains along the *c*-axis (Figure 1a). In the 1D

[Sb₆S₁₃] chains, the Sb(3)S₃ trigonal-pyramids acts as tridentate linker with a formation of [Sb₃S₇] semicub, whereas Sb(6)S₃ perform as bidentate node. The Sb(7)S₃ and Sb(8)S₃ trigonal bipyramids are assembled into a [Sb₂S₅] dimer via sharing one corner S atom. Two reverse parallel 1D [Sb₆S₁₃] chains are bridged by the above [Sb₂S₅] dimers and [(dienH)MnS₄] complexes on both sides via sharing S atoms into a 1D [(dienH)MnSb₈S₁₅]³⁻ anionic tube along the *c*-axis (Fig. 1). As far as we known, most of the thioantimonates trend to feature oligomer, 1D chain, 2D layer or 3D framework, and such 1D tube in compound **1** is still rare.

Viewed down the *c*-axis, the 1D anionic tube reveals small 1D channels consisting of [Sb₂Mn₂S₄] 8-membered ring, which has a nearly quadrangle cross-section with dimensions of approximately 3.86 × 4.68 Å. Such 1D [(dienH)MnSb₈S₁₅]³⁻ anionic tube feature parallel packing along the *a*- and *b*-axis (Figure 1b). The protonated [dienH₃] and dissociative H₂O molecules as charge-balancing agents or templated molecules are located among the space of 1D anionic tubes, forming extensive N–H···S and O–H···S hydrogen bonds with S atoms into a 3D H-bonding network structure. The N···S and O···S separations are in the range of 2.840-3.725 Å and 3.301-3.358 Å, respectively, which belong to the normal values.

Crystal Structure of 2. Compound **2** crystallizes in the monoclinic space group *P2/c* (No. 13) and its fundamental structure consists of discrete 1D [Mn(tren)]₂Sb₂S₈ ribbons, [Mn(teta)(H₂O)₂]²⁺ complexes and [SbS₄]³⁻ anions (Fig. 2). There are two crystallographically distinct Sb atoms, two Mn atoms in the asymmetric unit of compound **2**. All the Sb atoms are coordinated by four S²⁻ ions with tetrahedral coordination environments. The Sb-S bonds lengths and S-Sb-S angles fall in the range of 2.3144(13)-2.3840(10) Å and 107.81(5)-111.40(5)°, respectively, which indicate slight deviation from the ideal tetrahedral geometry. Hence, we easily conclude that all the Sb centers should be positive five oxidation states. The Mn(1) atom is firstly coordinated by four nitrogen atoms from two tren ligands to form a 1D [Mn(tren)]²⁺ complex chain, and two such neighboring 1D chains are further bridged by each pairs of Sb(1)S₄ tetrahedra via Mn-S bonds into 1D [Mn(tren)]₂Sb₂S₈ double chains along the *b*-axis

(Figure 2a). Hence, the Mn(1)²⁺ ion is coordinated by four N atoms and two terminal S atoms from two [SbS₄] tetrahedral with an octahedral environment, which is different from that of compound **1**. Each tren ligand works as a μ₃-bridging ligand bridging two Mn²⁺ ions in the 1D [Mn(tren)]²⁺ chains, and such coordinated mode is similar to that of [Ni₄(tren)₆][Mo₂O₂S₆]₄·nH₂O, in which the Ni²⁺ ions are bridged by tren ligands to form 1D zigzag [Ni₄(tren)₆]⁸⁺ chains.³⁵ The Mn-N and Mn-S bond lengths are in the range of 2.241(3)-2.404(3) Å and 2.5848(12)-2.7896(12) Å, respectively, which are accordance with those of compound **1**. The Mn(2) ion is also in a octahedral coordination geometry and surrounded by four nitrogen atoms from one tetra ligand and two oxygen atoms from two H₂O molecules. The above 1D [Mn(tren)]₂Sb₂S₈ double chains, [Mn(tetra)(H₂O)₂]²⁺ complexes and [SbS₄]³⁻ anions as well as H₃O⁺ ions are interconnected via N-H...S and O-H...S hydrogen bonds to form a 3D H-bonding network structure (Fig. 2).

The most prominent feature for compounds **1** and **2** are the diversiform coordination models and structural directing actions of organic amine ligands. In compound **1**, one dien ligand only affords two neighboring nitrogen atoms coordinating to Mn²⁺ ion as well as one terminal protonated amidogen, and another dien ligand is protonated acting as charge-balancing agent. As far as we known, the dien ligand is favor to *in situ* chelate transitional metals (Mn²⁺, Fe²⁺, Co²⁺ and Ni²⁺ ions) to form stabilized [TM(dien)₂]²⁺ complexes under solvothermal reaction, and only a very few example feature other models. For example, the dien ligand also only afford two nitrogen atoms chelating transitional metal ions in [Mn(dien)]MnSb₂S₅,³⁴ and [Co(dien)₂](H₂dien)Ge₂S₆ simultaneously contain saturated [Co(dien)₂]²⁺ complex and protonated [H₂dien]²⁺ cations.³⁶ Compound **2** simultaneously contains two types of tetradentate ligand of tren and tetra, and some other mixed amine ligands of chalcogenides has been reported including (tetraH)₂[Ln₂(tetra)₂(tren)₂(μ-Sn₂S₆)]Sn₂S₆ (Ln = Eu, Sm), [Co(dien)₂][Co(tren)SbS₄]₂·4H₂O, [Ni(tren)₂][Ni(tren)(en)]Sb₄S₈·nH₂O and [Ni(dien)(Htren)]Sb₄S₇, etc.³⁷

Optical Properties The optical properties of compounds **1** and **2** were studied by the solid-state diffuse-reflectance UV/Vis spectroscopy at room temperature. The absorption data was calculated from

the reflectance using the Kubelka-Munk function. As shown in Fig. 3, the optical band gaps obtained by extrapolation of the linear portion of the absorption edges are estimated as 1.81 and 2.23 eV for **1** and **2**, respectively, corresponding to their wine and yellow color. These absorptions can be assigned to the electronic excitation located at the anionic networks. The band gaps are compared with those of other thioantimonate, such as $[\text{Mn}_2\text{Sb}_2\text{S}_5(\text{N}_2\text{H}_4)_3]$ (2.09 eV) and $[\text{Ni}(\text{en})_3]\text{Sb}_4\text{S}_7$ (2.35 eV), etc.^{38,27}

Thermal Stabilities. The thermal stabilities of **1** and **2** were examined by thermogravimetric analyses (TGA) in N_2 atmosphere from 30 to 800 °C (Fig. 4). The TGA curves show that the compounds **1** and **2** both feature lower stabilities under heating condition. Compound **1** start to decompose at 30 °C and all long lose weight up to 600 °C with a final weight loss of 37.04 %, corresponding to the release of all organic-amine ligands, one H_2O and two H_2S as well as one Sb_2S_3 molecules (calcd. 36.37%). Compound **2** also feature consecutive decomposition from 30 °C to 350 °C with total weight loss of 42.13%, which is close to the calculated amount (42.05 %) of all amine ligands, H_2O molecules as well as a half of H_2S molecule. After lose the organic molecules, compound **2** continue to slowly lose weight and still do not achieve the balance to 800 °C.

Magnetic Properties. The magnetic susceptibilities of **1** and **2** were investigated on crystalline samples in the temperature range of 5-300 K under an applied field of 1000 Oe. They are plotted as $\chi_{\text{m}}T$ versus T ($\chi_{\text{m}}T$ is the magnetic susceptibility per Mn(ii) ion) for compounds **1** and **2** in Fig. 5. For compound **1**, the $\chi_{\text{m}}T$ product is equal to 4.20 $\text{emu mol}^{-1}\text{K}$ at 300 K, which is close to the spin-only value (4.375 $\text{emu mol}^{-1}\text{K}$) for a single high-spin Mn(II) ion. On lowering the temperature, the value of $\chi_{\text{m}}T$ is almost constant until approximately 45 K and then decreases at a faster rate, reaching a value of 3.45 $\text{emu mol}^{-1}\text{K}$ at 5 K. For compound **2**, $\chi_{\text{m}}T$ is equal to 4.64 $\text{emu mol}^{-1}\text{K}$ at 300 K, a little higher than the value for one isolated Mn(ii) ion. With lowering of the temperature, the value of $\chi_{\text{m}}T$ product decreases slightly to 3.45 $\text{emu mol}^{-1}\text{K}$ at 5 K. These results suggest the antiferromagnetic coupling between the Mn(II) ions in both **1** and **2**.

The temperature dependence of the molar susceptibility χ_{m} and $1/\chi_{\text{m}}$ for per Mn(ii) ion are also shown in Fig. 5. The calculated effective magnetic moments of compounds **1** and **2** at 300 K are 5.83 and 6.09

μ_B per Mn^{2+} ion, respectively, which is comparable with the calculated magnetic moment ($5.92 \mu_B$) for one Mn^{2+} ion. Both compounds **1** and **2** show the Curie–Weiss behavior in the temperature range of 5–300 K. The Curie–Weiss fit to the 5–300 K susceptibility data yield $C = 4.22$ and $4.72 \text{ emu}\cdot\text{K mol}^{-1}$, and $\theta = -1.52$ and -13.85 K for compounds **1** and **2**, respectively, where C and θ are the Curie and Weiss constants, respectively. The small negative Weiss contents also indicate the weak antiferromagnetic interactions and are consistent with the observed paramagnetic behavior down to a very low temperature. It should be noted that the amplitude of the Weiss constant of **1** is slightly smaller than that of **2**, which is consistent with the distances of closely adjacent Mn(II) ions in **1** and **2**. The nearest Mn(II)⋯Mn(II) distance is of 6.889 \AA in compound **1**. However, there are three kinds of Mn(II)⋯Mn(II) distances [Mn1⋯Mn1: 3.956 \AA and 7.924 \AA , and Mn2⋯Mn2: 7.924 \AA] in compound **2**, and one of them is shorter than that in **1**, creating the stronger antiferromagnetic coupling interaction in **2**.

Conclusions

In summary, two new organic–inorganic hybrid thioantimonate have been prepared with the presence of *in situ* formed manganese-amine complexes. Compound **1** features 1D $[(\text{dienH})\text{MnSb}_8\text{S}_{15}]^{3-}$ tubes and compound **2** contains 1D $[\text{Mn}(\text{tren})_2\text{Sb}_2\text{S}_8]$ ribbons, $[\text{Mn}(\text{teta})(\text{H}_2\text{O})_2]^{2+}$ complexes and $[\text{SbS}_4]^{3-}$ anions. The organic amines feature diversiform coordination models and structure-directing actions in the title compounds. In compound **1**, two dien ligands perform as partial coordination to Mn atoms and protonated cation, respectively, and compound **2** contains mixed tetradentate ligand of tren and tetra chelating amines. The present work further show that amine ligand is able to feature manifold structure-directing agents and stabilizing agents, and mixed template are favor to synthesize chalcogenides with new structural type. Research on this subject is in progress.

Acknowledgments

We thank the financial supports from the National Nature Science Foundation of China (Nos. 21101075 and 21201081); the Research Foundation for Excellent Young and Middle-aged Scientists of Shandong

Province (No. BS2011CL009 and BS2012CL008); China Postdoctoral Science Foundation funded project (No. 2012M521321); High Educational Science & Research Foundation of Shandong Province (No. J11LB52 and J13D58), Post Doctoral Innovation Project of Shandong Province (201303097), and Scientific Research and Technological Development Program of Jining City (No.20125014).

Supplementary Information

Electronic supplementary information (ESI) available: Crystallographic data in CIF format (CCDC numbers 961614 for **1**, 961615 for **2**), and tables of atomic coordinates and hydrogen bonds, IR spectrum and XRD powder patterns.

References

1. (a) J. Zhou, J. Dai, G. Q. Bian, C. Y. Li, *Coord. Chem. Rev.*, 2009, **253**, 1221–1247; (b) W. S. Sheldrick, M. Wachhold, *Coord. Chem. Rev.*, 1998, **176**, 211–322.
2. (a) M. C. Chen, L. H. Li, Y. B. Chen, L. Chen, *J. Am. Chem. Soc.*, 2011, **133**, 4617–4624; (b) M. C. Chen, L. M. Wu, H. Lin, L. J. Zhou, L. Chen, *J. Am. Chem. Soc.*, 2012, **134**, 6058–6060.
3. P. T. Wood, G. L. Schimek, J. W. Kolis, *Chem. Mater.*, 1996, **8**, 721–726.
4. (a) H. G. Yao, M. Ji, S. H. Ji, R. C. Zhang, Y. L. An, G. L. Ning, *Crys. Growth & Des.*, 2009, **9**, 3821–3824; (b) H. G. Yao, P. Zhou, S. H. Ji, R. C. Zhang, M. Ji, Y. L. An, G. L. Ning, *Inorg. Chem.*, 2010, **49**, 1186–1190.
5. K.-S. Choi, M. G. Kanatzidis, *Inorg. Chem.*, 2000, **39**, 5655–5662.
6. W. S. Sheldrick, *Dalton Trans.*, 2000, 3041–3052.
7. H.-O. Stephan, M. G. Kanatzidis, *J. Am. Chem. Soc.*, 1996, **118**, 12226–12227.

8. (a) J. Zhou, L. T. An, F. L. Hu, X. Liu, R. Q. Zhao, J. W. Lin, *Cryst. Eng. Comm.*, 2012, **14**, 5544–5551; (b) Y. L. Pan, J. F. Chen, J. Wang, Y. Zhang, D. X. Jia, *Inorg. Chem. Commun.*, 2010, **13**, 1569–1571; (c) J. J. Liang, J. Zhao, Q. Y. Jin, D. X. Jia, Y. Zhang, J. S. Gu, *J. Chem. Crystallogr.*, 2010, **40**, 975–980.
9. (a) J. Zhou, F. L. Hu, L. T. An, X. Liu, C. Y. Meng, *Dalton Trans.*, 2012, **41**, 11760; (b) D. X. Jia, Q. X. Zhao, Y. Zhang, J. Dai, J. L. Zuo, *Inorg. Chem.*, 2005, **44**, 8861–8867.
10. (a) J. Zhou, L. T. An, X. Liu, H. H. Zou, F. L. Hu, C. M. Liu, *Chem. Commun.*, 2012, **48**, 2537–2539.
11. (a) W. W. Tang, R. H. Chen, J. Zhao, W. Q. Jiang, Y. Zhang, D. X. Jia, *Cryst. Eng. Comm.*, 2012, **14**, 5021–5026; (b) J. Zhou, X. H. Yin, F. Zhang, *Cryst. Eng. Comm.*, 2011, **13**, 4806–4809.
12. (a) A. V. Powell, S. Boissière, A. M. Chippindale, *Chem. Mater.*, 2000, **12**, 182–187; (b) A. V. Powell, S. Boissière, A. M. Chippindale, *Dalton Trans.*, 2000, 4192–4195.
13. (a) X. Q. Wang, L. M. Liu, A. J. Jacobson, *J. Solid State Chem.*, 2000, **155**, 409–416; (b) A. V. Powell, R. Paniagua, P. Vaqueiro, A. M. Chippindale, *Chem. Mater.*, 2002, **14**, 1220–1224.
14. (a) P. Vaqueiro, A. M. Chippindale, A. R. Cowley, A. V. Powell, *Inorg. Chem.*, 2003, **42**, 7846–7851; (b) V. Spetzler, H. Rijnberk, C. Näther, W. Bensch, *Z. Anorg. Allg. Chem.*, 2004, **630**, 142–148; (c) A. Puls, M. Schaefer, C. Näther, W. Bensch, A. V. Powell, S. Boissière, A. M. Chippindale, *J. Solid State Chem.*, 2005, **178**, 1171–1181.
- 15 (a) V. Spetzler, C. Näther, W. Bensch, *J. Solid State Chem.*, 2006, **179**, 3541–3549; (b) M. L. Feng, D. N. Kong, Z. L. Xie, X. Y. Huang, *Angew. Chem. Int. Ed.*, 2008, **47**, 8623–8626; (c) J. L. Mertz, N. Ding, M. G. Kanatzidis, *Inorg. Chem.*, 2009, **48**, 10898–10900.
- 16 (a) Z. Rejai, H. Lümann, C. Näther, R. K. Kremer, W. Bensch, *Inorg. Chem.*, 2010, **49**, 1651–1657; (b) M. L. Feng, W. W. Xiong, D. Ye, J. R. Li, X. Y. Huang, *Chem. Asian J.*, 2010, **5**, 1817–1823;

- (c) M. L. Feng, C. L. Hu, K. Y. Wang, C. F. Du, X. Y. Huang, *Cryst. Eng. Comm.*, 2013, **15**, 5007–5011.
- 18 (a) K. Y. Wang, M. L. Feng, J. R. Li, X. Y. Huang, *J. Mater. Chem. A.*, 2013, **1**, 1709–1715; (b) A. V. Powell, R. J. E. Lees, A. M. Chippindale, *Inorg. Chem.*, 2006, **45**, 4261–4267.
- 19 (a) R. Stähler, B.-D. Mosel, H. Eckert, W. Bensch, *Angew. Chem. Int. Ed.*, 2002, **41**, 4487–4489; (b) W. Bensch, C. Näther, R. Stähler, *Chem. Commun.*, 2001, **5**, 477–478; (c) R. Stähler, C. Näther, W. Bensch, *Eur. J. Inorg. Chem.*, 2001, 1835–1840.
- 20 (a) R. Stähler, W. Bensch, *Z. Anorg. Allg. Chem.*, 2002, **628**, 1657–1662; (b) R. Kiebach, F. Studt, C. Näther, W. Bensch, *Eur. J. Inorg. Chem.*, 2004, 2553–2556; (c) D. X. Jia, Y. Zhang, J. Dai, Q. Y. Zhu, X. M. Gu, *J. Solid State Chem.*, 2004, **177**, 2477–2483.
- 21 (a) P. Vaqueiro, A. M. Chippindale, A. V. Powell, *Inorg. Chem.*, 2004, **43**, 7963–7965; (b) P. Vaqueiro, D. P. Darlow, A. V. Powell, A. M. Chippindale, *Solid State Ionics*, 2004, **172**, 601–605; (c) J. Zhou, G. Q. Bian, Y. Zhang, J. Dai, N. Cheng, *Z. Anorg. Allg. Chem.*, 2007, **633**, 2701–2705.
- 22 (a) R. J. E. Lees, Anthony V. Powell, A. M. Chippindale, *J. Phys. Chem. Solids*, 2007, **68**, 1215–1219; (b) M. Zhang, T. L. Sheng, X. H. Huang, R. B. Fu, X. Wang, S. M. Hu, S. C. Xiang, X. Tao Wu, *Eur. J. Inorg. Chem.*, 2007, 1606–1612.
- 23 (a) M. L. Feng, Z. L. Xie, X. Y. Huang, *Inorg. Chem.*, 2009, **48**, 3904–3906; (b) M. Zhang, T. L. Sheng, X. Wang, S. M. Hu, R. B. Fu, J. S. Chen, Y. M. He, Z. T. Qin, C. J. Shen, X. T. Wu, *Cryst. Eng. Comm.*, 2010, **12**, 73–76; (c) J. Zhou, X. H. Yin, F. Zhang, *Inorg. Chem.*, 2010, **49**, 9671–9676.
- 24 (a) B. Seidlhofer, J. Djamil, C. Näther, W. Bensch, *Cryst. Growth & Des.*, 2011, **11**, 5554–5560; (b) X. Liu, *Inorg. Chem. Commun.*, 2011, **14**, 437–439; (c) X. Liu, J. Zhou, *Inorg. Chem. Commun.*, 2011, **14**, 1286–1289.

- 25 (a) J. Zhou, L. T. An, *Cryst. Eng. Comm.*, 2011, **13**, 5924–5928; (b) B. Seidlhofer, V. Spetzler, C. Näther, W. Bensch, *J. Solid State Chem.*, 2012, **187**, 269–275; (c) K. Z. Du, M. L. Feng, L. H. Li, B. Hu, Z. J. Ma, P. Wang, J. R. Li, Y. L. Wang, G. D. Zou, X.Y. Huang, *Inorg. Chem.*, 2012, **51**, 3926–3928.
- 26 (a) W. W. Tang, C. Y. Tang, F. Wang, R. H. Chen, Y. Zhang, D. X. Jia, *J. Solid State Chem.*, 2013, **199**, 287–294; (b) J. Zhou, X. Liu, L. T. An, F. L. Hu, Y. H. Kan, R. Li, Z. M. Shen, *Dalton Trans.*, 2013, **42**, 1735–1742.
- 27 H.-O. Stephan, M. G. Kanatzidis, *Inorg. Chem.*, 1997, **36**, 6050–6057.
- 28 (a) H. Lümann, C. Näther, W. Bensch, *Z. Anorg. Allg. Chem.*, 2011, **637**, 1007–1012; (b) L. Engelke, C. Näther, P. Leisner, W. Bensch, *Z. Anorg. Allg. Chem.*, 2008, **634**, 2959–2965; (c) K. Möller, C. Näther, A. Bannwarth, W. Bensch, *Z. Anorg. Allg. Chem.*, 2007, **633**, 2635–2640.
- 29 (a) M. Schaefer, D. Kurowski, A. Pfitzner, C. Näther, Z. Rejai, K. Möller, N. Ziegler, W. Bensch, *Inorg. Chem.*, 2006, **45**, 3726–3731; (b) M. Schaefer, C. Näther, N. Lehnert, W. Bensch, *Inorg. Chem.*, 2004, **43**, 2914–2921.
- 30 (a) M. Schaefer, R. Stähler, W.-R. Kiebach, C. Näther, W. Bensch, *Z. Anorg. Allg. Chem.*, 2004, **630**, 1816–1822; (b) R. Kiebach, W. Bensch, R.-D. Hoffmann, R. Pöttgen, *Z. Anorg. Allg. Chem.*, 2003, **629**, 532–538; (c) M. Schaefer, L. Engelke, W. Bensch, *Z. Anorg. Allg. Chem.*, 2003, **629**, 1912–1918; (d) R. Stähler, W. Bensch, *Eur. J. Inorg. Chem.*, 2001, 3073–3078.
- 31 (a) Z. Q. Wang, G. F. Xu, Y. F. Bi, C. Wang, *Cryst. Eng. Comm.*, 2010, **12**, 3703–3707; (b) W. Bensch, C. Näther, M. Schur, *Chem. Commun.*, 1997, 1773–1774; (c) M. L. Fu, G. C. Guo, L. Z. Cai, Z. J. Zhang and J. S. Huang, *Inorg. Chem.*, 2005, **44**, 184–186.
- 32 G. M. Sheldrick, SHELXTL, Crystallographic Software Package, version 5.1; Bruker-Axs; Madison, WI, 1998.

- 33 K. Y. Wang, L. J. Zhou, M. L. Feng, X. Y. Huang, *Dalton Trans.*, 2012, **41**, 6689–6695.
- 34 L. Engelke, R. Stahler, M. Schur, C. Näther, W. Bensch, R. Pöttgen, M. H. Moller, *Z. Naturforsch., Teil B.*, 2004, **59**, 869-876.
- 35 J. Ellermeier, W. Bensch, *Z. Naturforsch., Teil B*, 2001, **56**, 611-623.
- 36 F. Zhang, X. H. Yin, X. Liu, J. Zhou, *Z. Anorg. Allg. Chem.*, 2011, **637**, 1388-1393.
- 37 (a) J. Zhou, X. Liu, L. T. An, F. L. Hu, W. B. Yan, Y. Y. Zhang, *Inorg. Chem.*, 2012, **51**, 2283–2290; (b) J. Lichte, H. Lühmann, C. Näther, W. Bensch, *Z. Anorg. Allg. Chem.*, 2009, **635**, 2021–2026; (c) H. Lühmann, Z. Rejai, K. Moller, P. Leisner, M.-E. Ordolff, C. Näther, W. Bensch, *Z. Anorg. Allg. Chem.*, 2008, **634**, 1687-1695.
- 38 Y. Liu, P. D. Kanhere, C. L. Wong, Y. F. Tian, Y. H. Feng, F. Boey, T. Wu, H. Y. Chen, T. J. White, Z. Chen, Q. C. Zhang, *J. Solid State Chem.*, 2010, **183**, 2644-2649.

Table 1. Crystal data and structure refinements for compounds **1** and **2**.

Compound	1	2
chemical formula	C ₈ H ₃₂ MnN ₆ OS ₁₅ Sb ₈	C ₂₄ H ₈₃ Mn ₄ N ₁₆ O ₅ S ₁₂ Sb ₃
fw	1738.24	1645.79
Space group	<i>P</i> -1 (No. 2)	<i>P</i> 2/ <i>c</i> (No. 13)
<i>a</i> (Å)	12.790(3)	15.529(2)
<i>b</i> (Å)	12.867(3)	7.9238(11)
<i>c</i> (Å)	13.616(3)	28.524(3)
α /°	112.894(2)	90
β /°	91.768(3)	119.779(5)
γ /°	92.612(3)	90
<i>V</i> (Å ³)	2059.2(8)	3046.4(7)
<i>Z</i>	2	2
Crystal size (mm)	0.08×0.08×0.04	0.10×0.08×0.06
<i>D</i> _{calcd} (g cm ⁻³)	2.803	1.794
Temp (K)	293(2)	293(2)
<i>h k l</i> ranges	±16, ±16, ±17	±20, ±10, ±36
μ (mm ⁻¹)	6.238	2.569
Reflections collected	24618	34546
Unique reflections	9417	6925
Reflections (<i>I</i> >2 σ (<i>I</i>))	7817	5388
GOF on <i>F</i> ²	1.006	1.079
R1, wR2 (<i>I</i> > 2 σ (<i>I</i>)) ^a	0.0445/0.0972	0.0304/0.0752
R1, wR2 (all data)	0.0544/0.1009	0.0492/0.1026
$\Delta\rho_{\max}$ (e/Å ³)	2.362	0.814
$\Delta\rho_{\min}$ (e/Å ³)	-1.265	-0.714

^a R1 = $\sum||F_o| - |F_c||/\sum|F_o|$, wR2 = $\{\sum w[(F_o)^2 - (F_c)^2]^2/\sum w[(F_o)^2]\}^{21/2}$

Table 2. Selected bond lengths (Å) for compounds **1** and **2**.

1			
Mn(1)-N(6)	2.263(9)	Sb(4)-S(10)	2.407(2)
Mn(1)-N(4)	2.348(9)	Sb(4)-S(11)	2.486(2)
Mn(1)-S(14)	2.567(3)	Sb(4)-S(13)	2.657(3)
Mn(1)-S(7)	2.644(3)	Sb(4)-S(5)#2	2.857(3)
Mn(1)-S(15)	2.652(3)	Sb(5)-S(13)	2.432(2)
Mn(1)-S(9)#1	2.726(3)	Sb(5)-S(8)	2.468(3)
Sb(1)-S(15)	2.421(2)	Sb(5)-S(3)	2.673(3)
Sb(1)-S(12)	2.525(2)	Sb(5)-S(10)	2.787(3)
Sb(1)-S(2)	2.760(3)	Sb(6)-S(14)	2.407(2)
Sb(1)-S(7)	2.837(3)	Sb(6)-S(7)	2.451(2)
Sb(2)-S(12)	2.462(2)	Sb(6)-S(8)#3	2.511(3)
Sb(2)-S(9)	2.524(2)	Sb(7)-S(4)	2.359(3)
Sb(2)-S(6)	2.591(3)	Sb(7)-S(3)	2.455(2)
Sb(2)-S(15)	2.872(2)	Sb(7)-S(1)#1	2.498(3)
Sb(3)-S(2)	2.426(3)	Sb(8)-S(5)	2.394(3)
Sb(3)-S(11)	2.492(3)	Sb(8)-S(6)	2.453(2)
Sb(3)-S(9)	2.557(2)	Sb(8)-S(1)	2.457(3)
2			
Mn(1)-N(3)	2.2416(7)	Mn(2)-O(2)	2.230(4)
Mn(1)-N(2)	2.247(3)	Mn(2)-O(1)	2.255(4)
Mn(1)-N(1)	2.276(4)	Mn(2)-N(8)	2.278(4)
Mn(1)-N(4)	2.4039(7)	Mn(2)-N(5)	2.282(4)
Mn(1)-S(1)	2.5845(12)	Mn(2)-N(6)	2.3012(7)
Mn(1)-S(1)#2	2.7896(13)	Mn(2)-N(7)	2.338(4)
Sb(1)-S(4)	2.3144(13)	Sb(2)-S(6)#1	2.3224(12)
Sb(1)-S(2)	2.3198(13)	Sb(2)-S(6)	2.3224(12)
Sb(1)-S(3)	2.3252(13)	Sb(2)-S(5)	2.3239(12)
Sb(1)-S(1)	2.3840(10)	Sb(2)-S(5)#1	2.3239(12)

Symmetry transformations used to generate equivalent atoms: For **1**: #1 $-x+1, -y+1, -z+1$; #2 $x, y, z-1$; #3 $x, y, z+1$; For **2**: #1 $-x+1, y, -z+1/2$; #2 $-x, y, -z+1/2$.

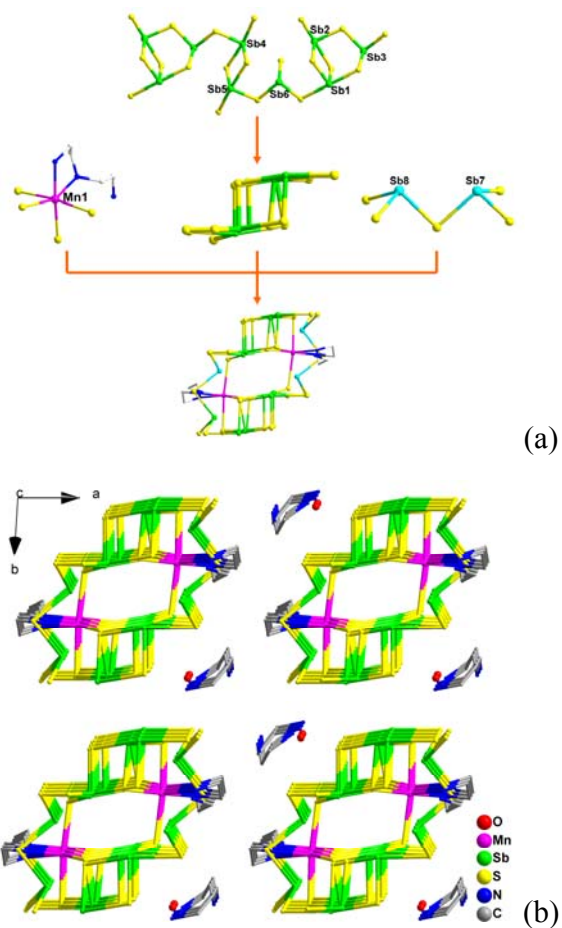


Fig. 1 Detailed view of the 1D $[(\text{dienH})\text{MnSb}_8\text{S}_{15}]^{3-}$ tube in compound **1** (a), and structure of compound **1** along the c -axis (b).

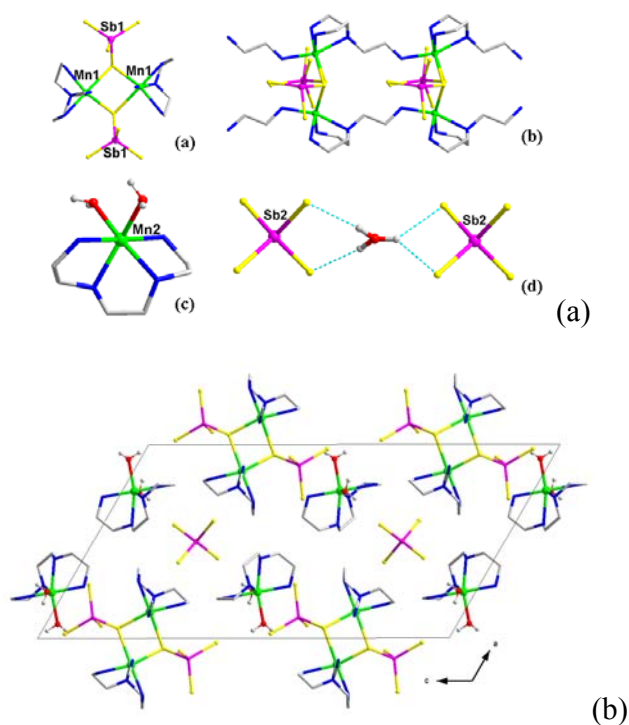


Fig. 2 Detailed view of the 1D $[\text{Mn}(\text{tren})]_2\text{Sb}_2\text{S}_8$ ribbons, $[\text{Mn}(\text{teta})(\text{H}_2\text{O})_2]^{2+}$ complexes and $[\text{SbS}_4]^{3-}$ anions in compound **2** (a), and the crystal structure of compound **2** along the b -axis (b).

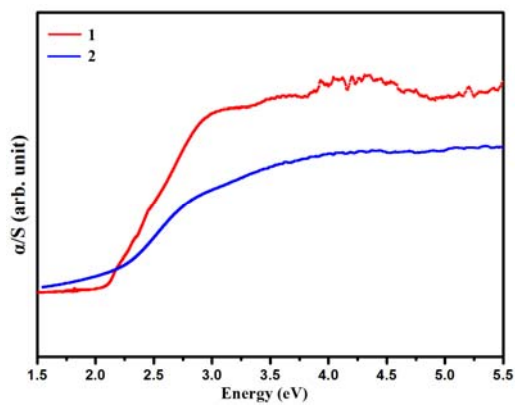


Fig. 3 Solid-state optical absorption spectra of compounds **1** and **2**.

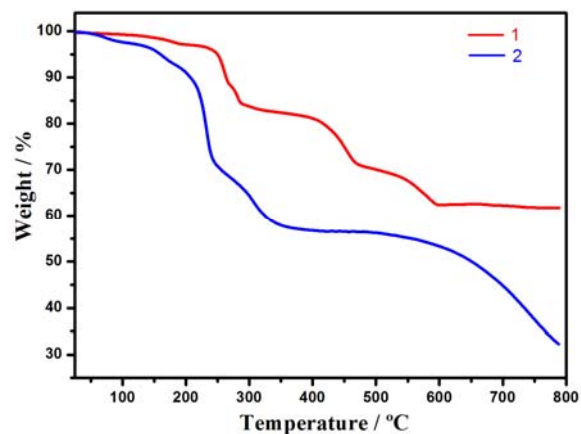


Fig. 4 Thermogravimetric curves for compounds **1** and **2**.

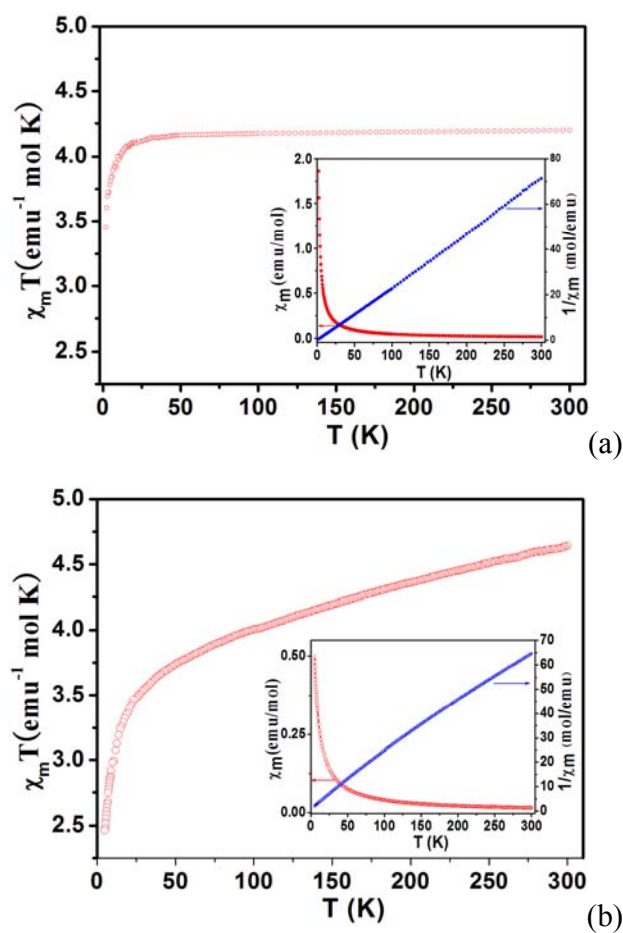
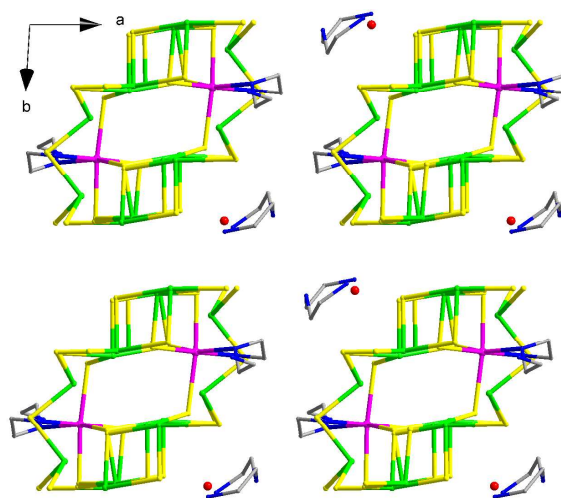


Fig. 5 Temperature dependence of the $\chi_m T$ curves for compounds **1** (a) and **2** (b). Inset: χ_m and $1/\chi_m$ vs T curves.

Two Manganese-amine complexes incorporated Thioantimonate Exhibiting Diversiform Structure-Directing Actions of Amine-ligands



Two manganese-amine complexes incorporated thioantimonate with diversified structure-directing actions of amine-ligands have been synthesized and characterized.